H, s), 3.80 (3 H, s), 17.0 (1 H, very broad s); ^{13}C NMR (CD_2Cl_2) 28.9, 37.8, 122.3.

Anal. Calcd for $C_6H_{13}F_3O_4N_2S$: C, 27.04; H, 4.92; F, 21.40; N, 10.52. Found: C, 27.02; H, 5.00; F, 17.39; N, 10.39.

Preparation of (NPYR)$_2$·HPF$_6$ (5). A solution of HPF_6·Et_2O (2.18 g, 9.9 mmol) in dichloromethane was prepared and to this was added 0.96 g (9.6 mmol) of NPYR. The resulting solution was filtered and diluted with ethyl acetate until a white precipitate had formed. The product was recrystallized three times from CH_2Cl_2/ethyl acetate to yield 0.19 g (6%) of product as white platelets, mp 118-122 °C dec: ^1H NMR (90 MHz, CD_2Cl_2) 2.19 (8 H, m), 3.87 (4 H, m), 4.34 (4 H, m), 17.0 (1 H, s); ^{13}C NMR ($CDCl_3$) 23.0, 24.0, 50.0, 53.0.

Anal. Calcd for $C_8H_{17}F_6N_4O_2P$: C, 27.75; H, 4.95; N, 16.18; P, 8.94. Found: C, 27.50; H, 5.14; N, 16.41; P, 9.20.

Preparation of (NSMOR)$_2$·HPF$_6$ (6). A solution of HPF_6·Et_2O (1.74 g, 7.9 mmol) in dichloromethane was mixed with 1.08 g of NSMOR (8.2 mmol) at room temperature and a stream of N_2 was passed over this solution until precipitation began. The cold CH_2Cl_2 was decanted and the residue was taken up in 10 mL of liquid sulfur dioxide. Filtration followed by the addition of CH_2Cl_2 and concentration to one-half volume led to the deposition of off-white platelets, which were again recrystallized from SO_2/CH_2Cl_2 to yield 0.46 g (27%) of white platelets, mp 81-83 °C dec: ^1H NMR (90 MHz, CD_2Cl_2) 1.9 (8 H, m), 4.29 (8 H, m), 17.8 (1 H, s); ^{13}C NMR (CD_2Cl_2) 25.7, 26.8, 47.5, 56.2.

Anal. Calcd for $C_8H_{17}F_6N_4O_2PS_2$: C, 23.41; H, 4.17; N, 13.65; P, 7.59; S, 15.62. Found: C, 23.13; H, 4.22; N, 13.56; P, 7.81; S, 15.90.

Acknowledgment. We thank G. Chmurny for collecting some of the NMR data. Research was supported in part by the National Institutes of Health under contract N01-CO-74102 to Program Resources, Inc.

Registry No. 2, 119819-03-3; 3, 119819-04-4; 4, 119819-05-5; 5, 114552-67-9; 6, 114552-68-0; NPIP·CF_3SO_3H, 119819-06-6; NPIP·$2CF_3SO_3H$, 119819-07-7; NPIP·HPF_6, 119819-08-8; NPYR·CF_3SO_3H, 119819-09-9; NDMA·CF_3SO_3H, 119819-10-2; NDCA·HPF_6, 119819-11-3; NPYR·$^3/_2CF_3SO_3H$, 119819-12-4.

Kinetic Study for Reactions of Nitrate Radical (NO_3·) with Substituted Toluenes in Acetonitrile Solution

Osamu Ito,* Seiji Akiho, and Masashi Iino

Chemical Research Institute of Nonaqueous Solutions, Tohoku University, Sendai, 980 Japan

Received October 27, 1988

The absolute rate constants for the reactions of the nitrate radical (NO_3·) with substituted toluenes in acetonitrile have been determined by the flash photolysis method. From the plots of the rate constants against the ionization energies, it was revealed that the reaction path for toluene derivatives with low ionization energies is different from that for toluene derivatives with high ionization energies. For toluene, a deuterium isotope effect was observed to be ca. 1.6, suggesting the direct hydrogen atom abstraction reaction; in this group, xylenes and *p*-chlorotoluene belong. For toluene derivatives with electron-withdrawing substituents, NO_3· may add to the phenyl rings followed by successive reactions. For both groups, linear correlations against the ionization energies with negative slopes show that NO_3· is highly electrophilic and that strong polar effects exist in the transition states of both reactions. For toluenes with methoxy groups, the electron-transfer reaction from methoxytoluene to NO_3· is a main initial path, since the transient absorption band due to the cation radical of methoxytoluene was detected.

Introduction

Photochemical reaction of $(NH_4)_2[Ce(NO_3)_6]$ with toluene derivatives ($ArCH_3$) in acetonitrile yields side-chain nitroxydation products in high yields.[1,2] For the initial

$$ArCH_3 \xrightarrow[\text{in acetonitrile}]{h\nu,\ (NH_4)_2[Ce(NO_3)_6]} ArCH_2ONO_2 \qquad (1)$$

step of this reaction, participation of NO_3· produced by the photolysis of $[Ce(NO_3)_6]^{2-}$ has been confirmed by flash

$$[Ce(IV)(NO_3)_6]^{2-} \underset{k_b}{\overset{h\nu}{\rightleftharpoons}} NO_3\cdot + [Ce(III)(NO_3)_5]^{2-} \qquad (2)$$

photolysis method.[3,4] Since NO_3· is known to be a strong oxidizing reagent as well as a hydrogen-atom abstracting reagent, the following two reactions would be anticipated:

$$NO_3\cdot + ArCH_3 \rightarrow ArCH_2\cdot + HNO_3 \qquad (3)$$

$$NO_3\cdot + ArCH_3 \rightarrow ArCH_3\cdot^+ + NO_3^- \qquad (4)$$

$$\downarrow$$

$$(ArCH_2\cdot + H^+)$$

It was presumed that the final product ($ArCH_2ONO_2$) was formed after further oxidation of $ArCH_2$· to $ArCH_2^+$ with $[Ce(NO_3)_6]^{2-}$ followed by the reaction with NO_3^-.[5]

For toluene derivatives with electron-donating substituents such as a methoxy group, the electron-transfer process (reaction 4) was confirmed by the laser flash photolysis method.[4] For toluene itself, however, there remains a possibility for the direct hydrogen-atom abstraction (reaction 3) with highly polar transition state. Furthermore, for toluene derivatives with electron-withdrawing substituents, the other initial reaction steps can be considered, since the high addition ability of NO_3· to phenyl π-bonds was assumed in the gas-phase reaction of NO_3· with phenol and furan.[6,7]

(1) Baciocchi, E.; Rol, C.; Sebastiani, G. V.; Serena, B. *Tetrahedron Lett.* **1984**, *25*, 1945.
(2) Baciocchi, E.; Del, Y.; Rol, C.; Sebastiani, G. V. *Tetrahedron Lett.* **1985**, *25*, 541.
(3) Ito, O. *Reprint of 8th IUPAC International Conference of Physical Organic Chemistry*; 1986, Tokyo; p 218.
(4) Baciocchi, E.; Giacco, T. D. Murgia, S. M.; Sebastiani, G. V. *J. Chem. Soc., Chem. Commun.* **1987**, 1246.
(5) Dincturk, S.; Ridd, J. H. *J. Chem. Soc., Perkin Trans. 2* **1982**, 961.

0022-3263/89/1954-2436$01.50/0

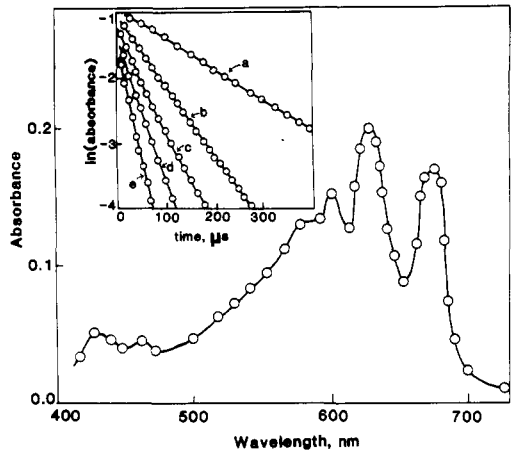

Figure 1. Transient absorption spectrum of $NO_3^\bullet$ in acetonitrile produced by flash photolysis of $K_2[Ce(NO_3)_6]$ (10^{-3} M); absorbances at 10 μs after flash are depicted. Insert: first-order decay of $NO_3^\bullet$ in presence of *p*-tolunitrile at 20 °C. [*p*-Tolunitrile]: (a) 0, (b) 16, (c) 32, (d) 64, and (e) 90 mM.

In this report, in order to clarify the interchanges in the reaction paths by the substituent in toluenes, the reaction rate constants for various toluene derivatives are evaluated by the flash photolysis method. We found that the initial reaction paths seem to vary with the ionization energies of the toluene derivatives. It is notable that kinetic data are useful to reveal a variety of the elemental reactions, which cannot be disclosed only from the product analysis yielding a single reaction product.

In addition, since the high reactivities of $NO_3^\bullet$ in solutions compared with those in gas phase have been suggested,[8] the origin of this difference was examined in terms of the solvent effect on the free-radical reactions.

Results and Discussion

Figure 1 shows the absorption spectrum of the transient species produced by the flash photolysis of $K_2[Ce(IV)(NO_3)_6]$ in acetonitrile solution. The transient absorption bands in the visible region (λ_{max} = 635 nm) were attributed to $NO_3^\bullet$.[9-12] Photodissociation (reaction 2) was confirmed to occur efficiently.

Insert of Figure 1 shows the decay rates of $NO_3^\bullet$ in the form of first-order plots. In acetonitrile without additive, the decay rate was slightly faster than that in aqueous solution. Since the decay of $NO_3^\bullet$ in aqueous solution was due to the back process of reaction 2 (k_b),[9,10] the increase in the decay rate in acetonitrile may be attributable to the acceleration of k_b by medium effect.

On the addition of appropriate amount of reactant (in the case of insert of Figure 1, *p*-tolunitrile), the slopes of the first-order plot, which are referred to the first-order decay rate constants ($k_{first\text{-}order}$), were increased with the concentrations of the additives. Spontaneous reaction in the dark was not observed for the additives such as toluene derivatives at a temperature lower than ca. 25 °C in acetonitrile.

In Figure 2, the pseudo-first-order plots ($k_{first\text{-}order}$ vs [additives]) for some toluene derivatives are shown; the slope yields the second-order rate constant. Although the extinction coefficients of $NO_3^\bullet$ in water (250 M^{-1} cm^{-1} at 635 nm)[9] and in the gas phase (10000 M^{-1} cm^{-1} at 665 nm)[12] were reported, that in acetonitrile was not reported. Assuming the extinction coefficient of 1000 M^{-1} cm^{-1} at 635 nm in acetonitrile, an initial concentration of $NO_3^\bullet$ was given to be ca. 10^{-6} M. This indicates that the addition of compounds above 10^{-5} M is enough to hold the pseudo-first-order relation. For *p*-xylene, the concentration of additive ((0.5–1) × 10^{-5} M) seems not to be excess, but decay kinetics obeys first-order kinetics not a second-order one.

The rate constants at 20 °C are summarized in Table I for some water-soluble substances whose rate constants in aqueous solution were reported.[10,11] In Table I, the rate

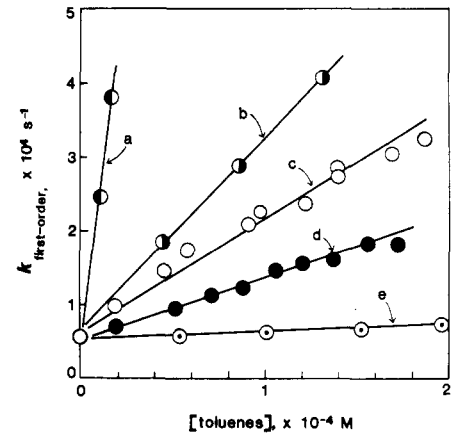

Figure 2. Pseudo-first-order plots: (a) *p*-xylene, (b) *p*-chlorotoluene, (c) toluene, (d) toluene-d_8, and (e) *m*-chlorotoluene.

Table I. Reaction Rate Constants[a] of $NO_3^\bullet$ with Various Compounds in Acetonitrile (20 °C), Aqueous Solution, and Gas Phase

entry no.	RH	$k \times 10^{-6}$, M^{-1} s^{-1} acetonitrile	aqueous	gas phase
1	CH_3OH	2.6	1.0[b] (0.21)[c]	
2	CH_3CH_2OH	6.7	3.9[b] (1.4)[c]	
3	$(CH_2)_4O$	55	16 (12)[c]	
4	$C_6H_5OCH_3$	3000 (10000)[d]	(3400)[c]	0.054[e]
5	C_6H_6	1.0		<0.021[e]
6	C_6H_5F	0.56		
7	C_6H_5CN	0.12		
8	$C_6H_5CH_3$	130 (130)[d]		0.020[e]
9	$C_6H_5CD_3$	80		
10	*m*-$CH_3C_6H_4CH_3$	730		0.12[e]

[a] Each value evaluated in this study (no suffix) may contain estimation error of ±5%. [b] Reference 10. [c] Reference 11. [d] Reference 4. [e] References 13 and 14.

Table II. Reaction Rate Constants (k at 20 °C) of $NO_3^\bullet$ with $XC_6H_4CH_3$ and Reported Ionization Energies (IE)

entry no.	X	$k \times 10^{-6}$, M^{-1} s^{-1}	IE,[a] eV
11	*p*-NO_2	0.23	9.50
12	*m*-NO_2	0.60	9.50
13	*p*-CN	0.22	9.38
14	*m*-CN	0.34	9.34
15	*p*-$CH_3C(O)$	0.25	9.14
16	*m*-F	5.2	8.90
17	*m*-Cl	6.4	8.83
8	H	130	8.76
18	*p*-Cl	280	8.69
10	*m*-CH_3	730	8.56
19	*p*-CH_3	>2000	8.44
20	*p*-OCH_3	>3000	8.25

[a] References 15 and 16.

(6) Carter, W. P. L.; Winer, A. M.; Pits, J. N., Jr. *Environ. Sci. Technol.* **1981**, *15*, 829.
(7) Atkison, R.; Aschmann, S. A.; Winer, A. M.; Carter, W. P. L. *Environ. Sci. Technol.* **1985**, *19*, 87.
(8) Ito, O.; Akiho, S.; Iino, M. *J. Phys. Chem.*, in press.
(9) Glass, R. W.; Martin, T. W. *J. Am. Chem. Soc.* **1970**, *92*, 5084.
(10) Dogliotti, L.; Hayon, E. *J. Phys. Chem.* **1967**, *71*, 3802.
(11) Neta, P.; Huie, R. E. *J. Phys. Chem.* **1986**, *90*, 4644.
(12) Sander, S. P. *J. Phys. Chem.* **1986**, *90*, 4135.

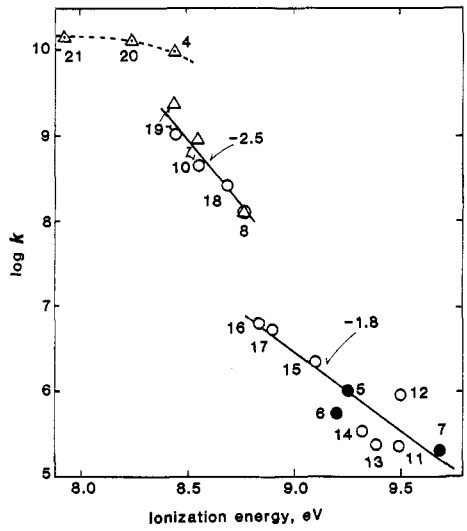

Figure 3. Plot of log k vs ionization energy; toluene derivatives (○) and benzene derivatives (●). Reported values for toluene derivaties (△) and anisole derivatives (▲).[4] Numbers refer to the entry numbers in Tables I and II; 21 is p-dimethoxybenzene.

constants for aromatic hydrocarbons are also summarized with the ones reported in gas phase.[13,14] The substituent effects of the rate constants for toluene derivatives are summarized in Table II, in which the ionization energies of these substances are added.[15,16]

As seen in Table I, the rate constants for alcohols and tetrahydrofuran in acetonitrile are larger than the corresponding values in aqueous solution by a factor of 2–5; from these compounds, $NO_3^•$ abstracts hydrogen atom at the α-position to the oxygen atom.[17] This difference may be attributed to the medium effect in hydrogen-atom transfer reaction; in general, the hydrogen bonds between the reactants and solvent may retard the rates of radical reactions.[18,19] The reaction rates for anisole and its derivatives are too fast to obtain the accurate rate constants by our flash photolysis method. Thus, only lower limits of the rate constants are obtained. For anisole, the medium effect seems to be not large; this is one piece of evidence for an electron-transfer reaction.[20]

For benzene, toluene, and xylene, the reported rate constants in the gas phase are considerably lower than the corresponding values in acetonitrile; as one of the reasons, the difference in the electronic structure of $NO_3^•$ between two phases has been proposed; in the gas phase, $NO_3^•$ has a regular triangle structure in which the minus charge equivalently delocalizes among three oxygens, whereas in polar solvents, $NO_3^•$ has an isosceles triangle structure in which an unpaired electron localizes on one oxygen atom.[8]

In Figure 2, the observed difference in the slopes between toluene and toluene-d_8 is larger than the experimental errors involved in this method. The deuterium

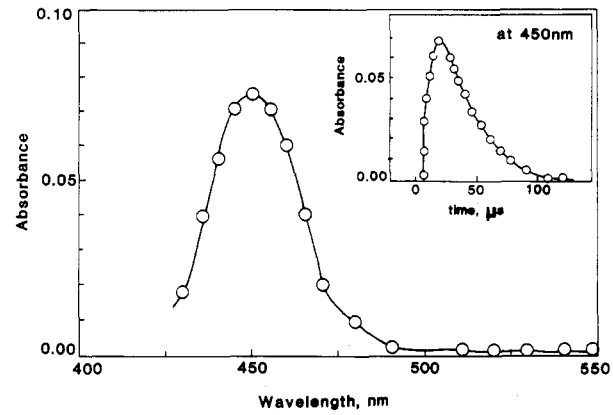

Figure 4. Transient absorption band observed by the flash photolysis of $K_2[Ce(NO_3)_6]$ (10^{-3} M) in presence of p-methylanisole (8×10^{-4} M); absorbances at 20 μs after flash. Insert: decay profile of absorption band at 450 nm.

kinetic isotope effect is 1.6, which is reasonable for primary deuterium kinetic isotope effect;[21] this indicates that $NO_3^•$ predominantly abstracts the hydrogen atom in the benzylic position. In the case of p-xylene, it was reported that the deuteirum-isotope effect was not observed;[4] since the rate constant for p-xylene is close to a diffusion-controlled limit in acetonitrile, the selectivity becomes low.

In Figure 3, the rate constants at 20 °C are plotted against the ionization energies; the reported rate constants in acetonitrile by laser flash photolysis[4] are also added to this figure. For xylenes, halves of the observed rate constants are plotted. The points can be divided into three groups. One is anisole derivatives, which have the rate constants greater than 3×10^9 M^{-1} s^{-1} (or 10^{10} M^{-1} s^{-1}).[4] For p-methylanisole, a new transient absorption band was observed instead of that of $NO_3^•$ by the flash photolysis of $K_2[Ce(NO_3)_6]$ in the presence of p-methylanisole (Figure 4). Although a 20-nm shift of the absorption peak from that of anisole cation radical was seen,[22] this absorption band was attributed to the cation radical of p-methylanisole. Electron transfer (reaction 4) was confirmed, which is reasonable because of high electron affinity of $NO_3^•$ (3.50 eV).[23]

The decay of the cation radical of p-methylanisole (insert of Figure 4) obeys the first-order kinetics, from which the deprotonation process of the cation radical forming the benzyl-type radical (reaction 3) is suggested. The first-order rate constant for this process was evaluated to be 2.1×10^4 s^{-1}. This value may be reasonable for the deprotonation process of the cation radical of p-methylanisole, since similar values were reported for the methylbenzenes having similar ionization potentials.[24] Thus, a following scheme was established:

$$NO_3^• + CH_3OC_6H_4CH_3 \xrightarrow{>3 \times 10^9\ M^{-1}s^{-1}} CH_3OC_6H_4CH_3^{•+} + NO_3^-$$

$$\downarrow 2.1 \times 10^4\ s^{-1}$$

$$(CH_3OC_6H_4CH_2^• + H^+) \quad (5)$$

The second group contains xylenes, toluene, and p-chlorotoluene whose ionization energies are in the range

(13) Atkison, R.; Plum, C. N.; Winer, C. A.; Pitts, J. N., Jr. *J. Phys. Chem.* **1984**, *88*, 2361.
(14) Atkison, R.; Carter, W. P. L.; Plum, C. N.; Winer, C. A.; Pitts, J. N., Jr. *Int. J. Chem. Kinet.* **1984**, *16*, 887.
(15) Kimura, K.; Katsumata, S.; Achiba, Y.; Yamazaki, T.; Iwata, S. *Handbook of He(I) Photoelectron Spectra of Fundamental Organic Molecules*; Halstead: New York, 1981.
(16) Closlowski, J.; Baranski, A.; Juska, T. *Tetrahedron* **1986**, *42*, 4549.
(17) Greatorex, D.; Hill, R. J.; Kemp, T. J.; Stone, T. J. *Trans. Faraday Soc.* **1974**, *70*, 216.
(18) Martin, J. C. In *Free Radicals*; Kochi, J. K., ed.; Wiley: New York, 1973; Chapter 20.
(19) Reichardt, C. *Solvent Effects in Organic Chemistry*; Verlag Chemie: Weinheim, 1979; Chapter 5.
(20) From anisole, polymeric products were produced after the electron transfer.[5] Similarly, from benzene, nitrobenzene was yielded;[5] the reaction mechanism, however, was not yet revealed.
(21) Russell, G. A. In *Free Radicals*; Kochi, J. K., Ed.; Wiley: New York, 1973; Chapter 7.
(22) O'Nell, P.; Steenken, S.; Schulte-Frohlinde, D. *J. Phys. Chem.* **1975**, *79*, 2773.
(23) Radzig, W. A.; Semirov, B. M. *Reference Data on Atoms, Molecules and Ions*; Springer-Verlag: Berlin, 1985.
(24) Sehested, K.; Holcman, J. *J. Phys. Chem.* **1978**, *82*, 1978.

of 8.45–8.80 eV. The rate constant of *p*-xylene is ca. 10 times smaller than that of anisole, which has the same ionization energy as *p*-xylene. Since the deuterium-isotope effect on the rate constants was observed for toluene and toluene-d_8, the direct hydrogen abstraction is attributed to this group.

$$NO_3^{\bullet} + XC_6H_4CH_3 \rightarrow HNO_3 + XC_6H_4CH_2^{\bullet} \quad (6)$$

$$(X = p\text{-}CH_3,\ m\text{-}CH_3,\ H,\ p\text{-}Cl)$$

The slope of this group in Figure 3 is −2.5; this indicates that $NO_3^{\bullet}$ is highly electrophilic. There are the contributions of the polar resonance structures like I and II to the transition state, which decreases the activation energy of the reaction.[21]

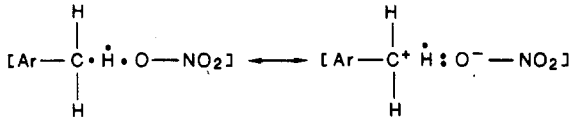

I II

The low activation energies for the reactions were confirmed by the small temperature variation of the rate constants, i.e., for toluene, the rate constant at −35 °C was 1.1×10^8 M^{-1} s^{-1}, from which the activation energy less than ca. 1 kJ/mol was evaluated.

The toluene derivatives with higher ionization energies than 8.80 eV belongs to the third group; the rate constant of *m*-chlorotoluene is ca. 10 times smaller than that of toluene, which has only a small (0.5 eV) ionization energy. The rate constants for toluene derivatives in this group also decreases linearly with an increase in the ionization energies. In this correlation line, the rate constants for substituted benzenes without the methyl group fit fairly good. The second-order rate constant for benzene is ca. $^1/_{200}$ of that of toluene. The electron-withdrawing substituents on the benzene ring such as F and CN reduce the reaction rates. For these compounds, the extra transient absorption band due to the cation radical was not observed in the visible region. These findings suggest that the addition reaction of $NO_3^{\bullet}$ to the double bonds in the benzene ring (reaction 7) is responsible to the decay of $NO_3^{\bullet}$.

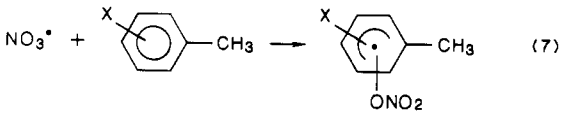

(7)

Even for toluene derivatives belonging to this group, it is reported that the side-chain nitroxydation also occurs similarly to toluene, although the yield was low.[1,2] This suggests that the benzyl-type radical is produced by the successive reaction. In the case of the reaction of $NO_3^{\bullet}$ with phenol in the gas phase,[6] since the addition–elimination mechanism was proposed, a similar mechanism (reaction 8) can be presumed for the toluene derivatives in this group.

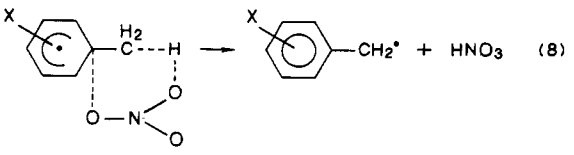

(8)

The slope of this group in Figure 3 is −1.8, which is less than that of the second group (−2.5). This tendency can be reasonably interpreted from the electron density of toluene derivatives, whereas it is anticipated that the polar contribution of the transition state for the abstraction reaction is smaller than the addition reaction.

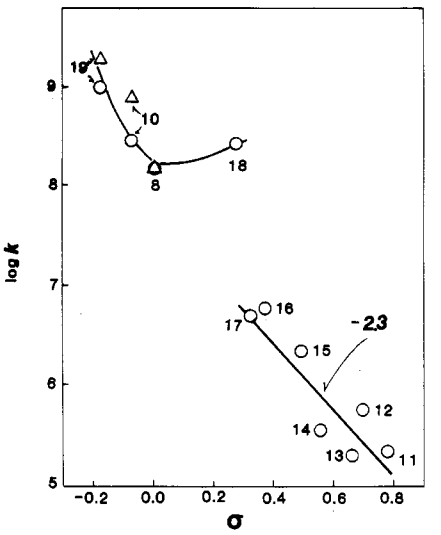

Figure 5. Hammett plot of log k vs σ: (○) values evaluated in this study, (△) reported values.[4] Numbers refer to the entry numbers in Tables I and II.

The Hammett plot against σ is shown in Figure 5. Compared with Figure 3, the points can also be divided into two groups. The group of toluenes with electron-withdrawing substituents shows a linear correlation with the slope of −3.2. This ρ value is more negative than the value of −2.3 for aromatic substitution reaction by isopropyl-$OCO_2^{\bullet}$, which is one of the highest electrophilic radicals.[25] The group of xylenes, toluene, and *p*-chlorotoluene shows an upward deviation from the extrapolated line of electron-poor toluene derivatives. These relatively electron-rich toluenes show a V-shaped correlation. This V-shaped correlation was frequently observed for the hydrogen-atom abstraction by the free radicals, to which the resonance factor contributes. It is noticeable that interchange of the reaction modes can be clearly shown from the correlation with the ionization energies (Figure 3) rather than the Hammett plot (Figure 5).

In Figure 3, a reaction-mechanistic break between toluene derivatives with ionization energies of about 8.75 eV was found. Such a interchange of the reaction modes in the narrow ionization energy region has not been reported. This may be caused by the high reactivities of $NO_3^{\bullet}$ for various reaction modes such as electron transfer, hydrogen-atom abstraction, and addition to the double bond. Furthermore, $NO_3^{\bullet}$ has high sensitivity to the electron densities of the reactants. The electronic structure of $NO_3^{\bullet}$ may be easily changeable by the approach of the reactants with different electron densities. This may be the same origin to the big medium effect on the reactivities observed especially between in acetonitrile and in gas phase.

Experimental Section

Materials. $K_2[Ce(IV)(NO_3)_6]$ was prepared from the ammonium salt by the action of KOH. Commercially available toluene derivatives and other reagents were purified by repeated distillation or by recrystallization. Toluene-d_8 (Aldrich Chemical Ltd.; minimum isotope purity of >99 atom %)) was used as received. Acetonitrile used as a solvent was purified by distillation after the reflux with P_2O_5 under nitrogen gas.

Apparatus. Flash photolysis apparatus was of standard design with xenon flash lamps (Xenon Corp. N-851C), which gave 8 μs of flash duration and 100-J input energy. The light filters were selected so as to photolyze the radical source (longer wave length

(25) Kovacic, P.; Reid, C. G.; Kuntz, M. K. *J. Org. Chem.* **1969**, *34*, 3302.

than 350 nm). The absorbances of Figures 1, 2, and 4 are observed values in the flash photolysis cell with 10 cm of optical path. Temperature of solution was controlled by immersing the flash photolysis cell in a bath cooled by low-temperature methanol in the vessel with windows.

Procedure. On the addition of toluene, the dark reaction was monitored by the absorption band of $K_2[Ce(NO_3)_6]$ at 350 nm in order to check the reactions of aromatic compounds with $K_2[Ce(NO_3)_6]$. Under the conditions of temperature (<20 °C) and concentrations of toluene ($<10^{-3}$ M) and $K_2[Ce(NO_3)_6]$ ($<10^{-3}$ M), the consumptions of both materials were not observed in acetonitrile. For each flash exposure, a freshly prepared solution was used. The presence of oxygen in solution did not affect the decay rate of $NO_3^{\bullet}$; all measurements were performed in aerated solution.

Acknowledgment. We are thankful to Grant-in-Aid for Scientific Research (No. 62540314 and 63550676) from the Ministry of Education, Science and Culture of Japan. We also express our deep thanks to Dr. Kingo Itaya of Tohoku University for his useful discussion.

Registry No. CH_3OH, 67-56-1; CH_3CH_2OH, 64-17-5; $(CH_2)_4O$, 109-99-9; $C_6H_5OCH_3$, 100-66-3; C_6H_6, 71-43-2; C_6H_5F, 462-06-6; C_6H_5CN, 100-47-0; $C_6H_5CH_3$, 108-88-3; D_2, 7782-39-0; *m*-$CH_3C_6H_4CH_3$, 108-38-3; *p*-$NO_2C_6H_4CH_3$, 99-99-0; *m*-$NO_2C_6H_4CH_3$, 99-08-1; *p*-$CNC_6H_4CH_3$, 104-85-8; *m*-$CNC_6H_4CH_3$, 620-22-4; *p*-$CH_3C(O)C_6H_4CH_3$, 122-00-9; *m*-$FC_6H_4CH_3$, 352-70-5; *m*-$ClC_6H_4CH_3$, 108-41-8; *p*-$ClC_6H_4CH_3$, 106-43-4; *p*-$CH_3C_6H_4CH_3$, 106-42-3; *p*-$CH_3OC_6H_4CH_3$, 104-93-8; $K_2[Ce^{IV}(NO_3)_6]$, 17126-44-2; $NO_3^{\bullet}$, 12033-49-7; *p*-methylanisole, 38144-90-0.

Lewis Acid Promoted Decomposition of Substituted 1,3,2λ⁵-Dioxaphospholanes: Kinetic and Thermodynamic Studies

William T. Murray and Slayton A. Evans, Jr.*

The William Rand Kenan, Jr., Laboratories of Chemistry, CB 3290, The University of North Carolina, Chapel Hill, North Carolina 27599-3290

Received December 15, 1988

The kinetics of Lewis acid mediated decomposition of a series of substituted 1,3,2λ⁵-dioxaphospholanes, prepared by transphosphoranylation of 1,2-diols with diethoxytriphenylphosphorane (DTPP), is reported. The rate data, obtained from ^{31}P NMR spectroscopic measurements, emphasize the influence of (i) variations in the coordination potential (i.e., cationic charge) of the Lewis acids, (ii) methyl group substitution at C-4 and C-5 in the 1,3,2λ⁵-dioxaphospholanyl substructure, and (iii) changes in solvent polarity. Also, the propensity for 1,2-hydride migratory processes attending conformationally restricted *bicyclic* 1,3,2λ⁵-dioxaphospholanes versus epoxide formation from the collapse of simple *cyclic* 1,3,2λ⁵-dioxaphospholanes were examined. The results are best explained by invoking a "site-selective" coordination by the catalyst to one of the "ethereal" oxygens within the 1,3,2λ⁵-dioxaphospholanyl moiety initiating P–O bond cleavage and ultimately affording the requisite betaine intermediate(s). Methyl substitution on the 1,3,2λ⁵-dioxaphospholanyl hydrocarbon backbone decreases the rate of P–O bond cleavage, and the 1,2-hydride migratory process within conformationally rigid bicyclic 1,3,2λ⁵-dioxaphospholanes requires ca. 2.0 kcal/mol more energy than the decomposition of the *monocyclic* 1,3,2λ⁵-dioxaphospholanes via 3-exo-tet cyclization to the respective cyclic ethers. Mechanistic implications of various reactions are discussed.

Introduction

Recent research from our laboratories has demonstrated that both cyclic and acyclic dioxaphosphoranes are useful reagents for preparing a variety of heterocycles, including cyclic ethers,[1-6] cyclic sulfides,[4,5,7] chiral aziridines,[4,5,8] and diastereomeric 1,4-oxathianes.[9] The transphosphoranylations of, particularly, mono- and disubstituted 1,2-diols with diethoxytriphenylphosphorane (DTPP) give the requisite 1,3,2λ⁵-dioxaphospholane intermediates, which subsequently decompose to the corresponding oxiranes in high yields (40 °C, 48 h). By contrast, the sterically more congested, tri- and tetrasubstituted 1,3,2λ⁵-dioxaphospholanes from the condensation of the corresponding 1,2-diols with DTPP require higher reaction temperatures (80–100 °C, 48 h) for initiating *any* appreciable reaction. In fact, these higher temperatures cause a diminution in the yield of the epoxides and accelerate production of a variety of side products. In this light, we reported that lithium bromide (LiBr) catalyzes the smooth and rapid cyclodehydration of these substituted 1,2-diols, through the corresponding 1,3,2λ⁵-dioxaphospholanes, giving remarkably high yields of the epoxides at ambient temperature while suppressing formation of the side products.[10]

A mechanistic rationale for oxaphosphorane-promoted cyclodehydration of a 1,2-diol is presented in Scheme II. Transphosphoranylation of vicinal diols with DTPP produces the intermediate 1,3,2λ⁵-dioxaphospholanes, **1a** and **1b**, which undergo rapid Berry pseudorotation and afford time-averaged NMR resonances (^{31}P δ −35 to −50 ppm).[11]

(1) Robinson, P. L.; Barry, C. N.; Kelly, J. W.; Evans, S. A., Jr. *J. Am. Chem. Soc.* **1985**, *107*, 5210–9.
(2) Bass, S. W.; Barry, C. N.; Robinson, P. L.; Evans, S. A., Jr. *Phosphorus Chemistry: Proceedings of the 1981 International Conference*; Quin, L. D., Verkade, J. G., Eds; *ACS Symposium Series* **1981**, *171*, 165.
(3) Robinson, P. L.; Bass, S. W.; Jarvis, S. E.; Evans, S. A., Jr. *J. Org. Chem.* **1983**, *48*, 5396.
(4) Kelly, J. W.; Evans, S. A., Jr. *J. Org. Chem.* **1986**, *51*, 4473.
(5) Kelly, J. W.; Evans, S. A., Jr. *J. Org. Chem.* **1986**, *51*, 5490.
(6) Robinson, P. L.; Evans, S. A., Jr. *J. Org. Chem.* **1985**, *50*, 3860.
(7) Robinson, P. L.; Kelly, J. W.; Evans, S. A., Jr. *Phosphorus Sulfur* **1987**, *31*, 59–70.
(8) Kelly, J. W.; Eskew, N. A.; Evans, S. A., Jr. *J. Org. Chem.* **1986**, *51*, 95–7.
(9) Murray, W. T., Kelly, J. W.; Evans, S. A., Jr. *J. Org. Chem.* **1987**, *52*, 525–9.
(10) Murray, W. T.; Evans, S. A., Jr. *Nouv J. Chem.*, in press.

0022-3263/89/1954-2440$01.50/0